Acta Chemica Scandinavica, 1997: 51: 249–258
Printed in UK – all rights reserved

ACTA
CHEMICA SCANDINAVICA
ISSN 0904–213X

In-situ Investigation of Magnesium Aluminophosphate Synthesis by Synchrotron X-Ray Powder Diffraction

A. Nørlund Christensen,*[,a] P. Norby[b] and J. C. Hanson[b]

[a]Department of Inorganic Chemistry, Aarhus University, DK-8000 Aarhus C, Denmark and [b]Chemistry Department, Brookhaven National Laboratory, Upton, New York 11973, USA

Christensen, A. N., Norby, P. and Hanson, J. C. 1997. *In-situ* Investigation of Magnesium Aluminophosphate Synthesis by Synchrotron X-Ray Powder Diffraction. – Acta Chem. Scand. 51: 249–258. © Acta Chemica Scandinavica 1997.

Time-resolved synchrotron X-ray powder diffraction was used to study synthesis of magnesium substituted aluminophosphates. Four organic template molecules were applied, which resulted in different reaction products. Triethylamine: MAPO-5 and MAPO-47. Di-*n*-propylamine: MAPO-39 and MAPO-46. Tripropylamine: MAPO-36. Tetramethylammonium hydroxide: MAPO-20. Some synthesis passed through the formation of precursor phases. A precursor observed in the lower temperature range of the synthesis was $Mg(H_2O)_4[Al(PO_3OH)OH](H_2O)_2$.

A study of aluminophosphate-based molecular sieves was reported by Wilson *et al.*,[1] and since then a large number of aluminophosphate-based framework structure compounds have been discovered. Among these are the MAPOs, where the aluminium may be partly substituted by the metals Mg, Mn and Co. The substitution of the Al^{3+} ion with the Me^{2+} ions in the zeolite like framework results in a greater acidity and stronger catalytic activity of the compounds compared to that of the not substituted aluminophosphates with the same type of framework structure.

The aluminophosphate-based molecular sieves are made at hydrothermal conditions from amorphous aluminophosphate gels containing organic template molecules. The same framework structure can often be made using different organic molecules and using the same organic molecule and slight variations in the synthesis conditions as composition, pH and aging of the gel, and temperature and time of the hydrothermal reaction, may result in different framework structures.[2] Akolekar and Kaliaguine[3] thus reported that the template di-*n*-propylamine in hydrothermal synthesis with magnesium aluminophosphate gels could yield the compounds MAPO-11, MAPO-39, MAPO-43, MAPO-46 and MAPO-50. The MAPO nomenclature is taken from Ref. 4.

Although several papers have been published on the synthesis of metal substituted aluminophosphates, little is known about the rate of formation in the hydrothermal reaction to produce the MAPOs with molecular sieve properties. Only one *in-situ* X-ray synchrotron powder diffraction investigation has been reported on the synthesis of CoAPO-5.[5] For this reason it was decided to investigate further the formation of MAPOs by *in-situ* X-ray synchrotron powder diffraction using Mg substitution and the templates triethylamine, which can yield MAPO-5 and MAPO-47,[6] di-*n*-propylamine and tripropylamine, which yields MAPO-36,[7,8] and the organic structure directing agent tetramethylammonium hydroxide and tripropylamine, which was used in the synthesis of MAPO-20.[9]

Experimental

The chemicals used in the synthesis of the MAPOs were the following: pseudo-boehmite (catapal B, Vista Chemical Co.), MgO (made from $MgCO_3$ Merck), $MgSO_4 \cdot 7H_2O$ (Merck), $Mg(CH_3COO)_2 \cdot 4H_2O$ (Aldrich), H_3PO_4, 85% (Merck), NaOH (Merck), triethylamine (Aldrich), di-*n*-propylamine (Aldrich), tripolylamine (Aldrich) and tetramethylammonium hydroxide (Aldrich).

Experiments with the use of organic templates. For each organic template a charge was prepared sufficiently large for all syntheses and diffraction experiments performed. The quantities used in the preparation of the gels are listed in Table 1 as molar ratios. The procedure for a preparation of a gel is as follows with the first gel listed in Table 1 as an example: 4.93 g magnesium sulfate was dissolved in 30 ml deionized water and this solution was added to 23.06 g 85% phosphoric acid. The mixture was stirred for 15 min, and then with continuous stirring

* To whom correspondence should be addressed.

Table 1. Composition of MAPO-gels used for *in-situ* experiments at NSLS. Molar ratios are listed.

Name of gel	Template	Template	Na_2O	MgO	Al_2O_3	P_2O_5	H_2O
MAPO-A gel	Triethylamine	1.48	0.017	0.20	1.02	1.00	27.75
MAPO-B gel	Di-*n*-propylamine	1.48		0.20	1.02	1.00	25.00
MAPO-C gel	Di-*n*-propylamine	2.00		0.30	0.85	1.00	25.00
MAPO-D gel	Tripropylamine	1.91		0.17	0.96	1.00	25.20
MAPO-E gel	Tetramethylammonium hydroxide	2.19	HCl 0.21	0.29	0.81	1.00	31.91

In preparation of the gels A and B, $MgSO \cdot 7H_2O$ was used, for the gels C, D and E $Mg(CH_3COO)_2 \cdot 4H_2O$ was applied.

14.04 g catapal B was added in small quantities and the gel so formed was stirred until homogeneous. 15.15 g triethylamine was then added dropwise, and finally a minor volume of a weak sodium hydroxide solution (0.8 g in 30 ml deionized water) was added dropwise until the pH of the gel was 5 as measured with indicator strips. To obtain homogeneity the gel was further stirred for 1 to 2 h, and the charge so obtained was stored at room temperature in a polyethylene flask.

Preliminary hydrothermal experiments were made with samples of the gels charged in glass or Teflon containers in pressure vessels at the experimental conditions listed in Table 2. The crystalline reaction products were washed with water and dried at room temperature, and X-ray powder patterns were recorded with a Stoe diffractometer using $CuK\alpha_1$ radiation and a position-sensitive detector. The reaction products were identified using the JCPDS data base and the results are listed in Table 2.

The *in-situ* synchrotron X-ray powder diffraction investigation of the samples were made at the Huber diffractometer at beam line X7B at NSLS, Brookhaven National Laboratory. The samples were kept in 0.5 and 0.7 mm diameter quartz capillaries at an internal pressure of up to 45 atm, and the capillaries were heated with a stream of hot air. A Fuji imaging plate system was used to record the powder patterns. The wavelengths used were $\lambda = 1.2571(1)$ Å for the MAPO-A and -B gel experiments, and $\lambda = 1.2104(1)$ Å for the MAPO-C, -D and -E gel experiments, respectively. Bragg reflections out to $\sin\theta/\lambda = 0.45$ were typically recorded, and crystalline compounds formed were identified from their X-ray powder patterns. Further details of the experimental arrangements have been reported previously.[10]

Table 2. Preliminary heat treatments (hydrothermal) of MAPO-gels.

Gel	Aging time[a]/ days	Hydrothermal conditions		Product
		T/°C	*t*/h	
MAPO-A	73	90	24	Mg-sinkankasite
	1	100	24	MAPO-47
	4	120	24	MAPO-47
	17	150	48	MAPO-47
	2	172	24	MAPO-47
MAPO-B	56	90	24	Mg-sinkankasite
	2	150	48	MAPO-39
MAPO-C	98	200	24	MAPO-39
MAPO-D	92	90	24	MAPO-36
	95	120	24	MAPO-36
	98	200	24	MAPO-36
MAPO-E	35	90	24	MAPO-20
	69	120	48	MAPO-20
	75	150	48	MAPO-20
	90	180	48	MAPO-20

[a] Aging time at room temperature prior to heat treatment.

Results and discussion

Preliminary hydrothermal experiments.

MAPO-A gel. This gel has the same $MgO : Al_2O_3$ ratio as the gel MG-10 used by Shea *et al.*[6] in the synthesis of the magnesium-substituted MAPO-5 but has a lower water content. They observed MAPO-47 as an impurity in some of the synthesis. The gel gave in hydrothermal synthesis (Table 2) MAPO-47 as the product at temperatures from 100 to 172 °C. After 2.5 months of ageing of the gel at room temperature, it yielded on heating to 90 °C for 24 h a crystalline product with a powder pattern very similar to that of MnAl $(PO_3OH)_2OH \cdot 6H_2O$, JCPDS card no. 42-597. This compound is the mineral sinkankasite and is according to a recent crystal structure investigation $Mn(H_2O)_4[Al(PO_3OH)_2OH](H_2O)_2$ and has a sheet structure.[11] Mg^{2+} and Mn^{2+} are rather similar in ionic radii, and it is assumed that the crystalline product is $Mg(H_2O)_4[Al(PO_3OH)_2OH](H_2O)_2$. It will in the following then be called Mg-sinkankasite. The X-ray pattern of the compound is displayed in Fig. 1, which also shows the calculated powder pattern using the model of Ref. 11 and the program LAZYPULVERIX.[12]

MAPO-B gel. This gel has a $MgO : Al_2O_3$ ratio smaller than in the gel batch A, used by Akolekar and Kaliaguine[7] in the synthesis of MAPO-46, and also has a smaller di-*n*-propylamine and water content than that gel. In heat treatments at 90 °C the gel gave Mg-sinkankasite, and in hydrothermal synthesis at 150 °C it gave MAPO-39 (Table 2).

MAPO-C gel. The gel has the same di-*n*-propylamine : $MgO : Al_2O_3 : P_2O_5$ ratio as the gel batch D, Ref. 7, but has a smaller water content. In hydrothermal

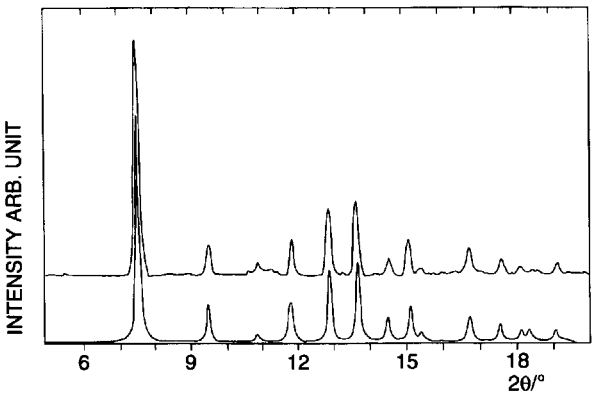

Fig. 1. Observed X-ray powder pattern, upper curve, and calculated X-ray powder pattern, lower curve, of Mg-sinkankasite. Unit-cell paramters $a=9.504$, $b=9.844$, $c=6.860$ Å, $\alpha=107.84$, $\beta=98.77$, $\gamma=98.79°$, space group $P\bar{1}$.

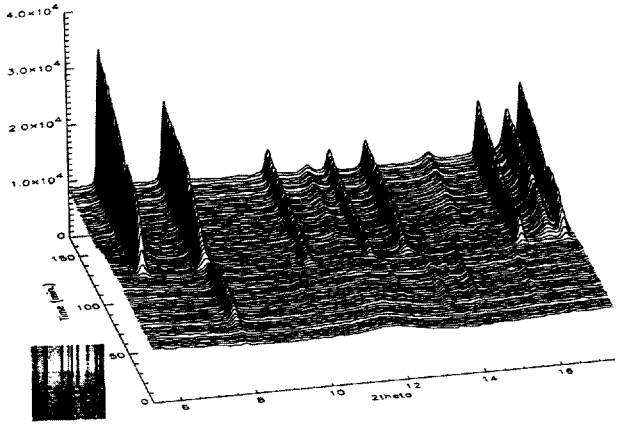

Fig. 2. Patterns of the MAPO-A gel heated from 25 to 200 °C for 120 min followed by 200 °C for 60 min. The precursor phase Mg-sinkankasite is formed and consumed at 120 °C where the formation of MAPO-5 and MAPO-47 starts. The rate of formation of MAPO-5 is greater than that of MAPO-47. The eight sharp Bragg reflections of the reaction product are from left to right: Second, fifth and seventh, the 101, 021 and 211 reflections of MAPO-47, respectively, and the remaining the 100, 110, 200, 212 and 002 reflections of MAPO-5, respectively.

synthesis at 200 °C (Table 2) the gel gave MAPO-39 as the reaction product.

MAPO-D gel. The gel has almost the same tripropylamine: $MgO:Al_2O_3:P_2O_5$ ratio as the gel batch A used by Akolekar[8] in the synthesis of MAPO-36, but has a smaller water content. The reaction product with the gel in hydrothermal synthesis at 120 and 200 °C is MAPO-36 (Table 2).

MAPO-E gel. This gel has a smaller MgO: Al_2O_3 ratio than the gel used by Barrie and Klinowski[13] to synthesise MAPO-20. In heat treatment at 90 °C and in hydrothermal synthesis at 120 and 180 °C (Table 2) the reaction product was MAPO-20.

In-situ *diffraction experiments.*

MAPO-A gel. Figure 2 shows the powder patterns obtained in heating the gel from 25 to 200 °C with a constant heating rate of 1.5 °C min^{-1}, after which the sample was kept at 200 °C for 60 min. At 25 °C the gel is X-ray amorphous and during heating the precursor phase Mg-sinkankasite is formed. At approximately 120 °C the precursor phase disappears, and the Bragg reflections from two reaction products appear, MAPO-47 and MAPO-5. The growth rate of MAPO-5 is faster than that of MAPO-47. The two molecular sieves have the following structure: MAPO-5 has the $AlPO_4$-5 framework which is hexagonal, space group $P6_{22}$ with $a=13.7$ Å and $c=8.4$ Å. MAPO-47 has the chabazite structure which is rhombohedral, space group $R\bar{3}m$ with $a=b=c=9.45$ Å and $\alpha=\beta=\gamma=94.0°$, and using hexagonal setting, the unit-cell parameters are $a=13.3$ Å, $c=15.1$ Å.

Figures 3A, 3B and 3C show powder patterns of gels heated rapidly to 130, 150, and 180 °C, respectively, and then kept at these temperatures for 2 h. At 180 °C (C) the rate of formation of MAPO-5 is greater than that of MAPO-47, and the two compounds are formed in approximately equal quantities. At 150 °C (B) the rate of formation of MAPO-5 is still greater than that of MAPO-47, but the quantity formed of MAPO-47 is greater than that of MAPO-5. At 130 °C (A) MAPO-5 is only formed in minor quantities, and MAPO-47 is the main reaction product. In Ref. 6 the hydrothermal synthesis were made at 150–190 °C for approximately 20 h and these syntheses produced MAPO-5 with minor impurities of MAPO-47. Synthesis performed at lower temperatures may well have resulted in large quantities of MAPO-47 as impurity, and in the preliminary hydrothermal experiments made in this work MAPO-47 was the main crystalline reaction product obtained from 120 to 172 °C.

The growth rate of the two compounds MAPO-5 and MAPO-47 can be visualized in a plot of Bragg intensities of selected reflections vs. time. Figure 4 displays the integrated intensities of MAPO-5 and MAPO-47 Bragg reflections at the temperatures 180, 150 and 130 °C, respectively. The growth rate of MAPO-5 is faster than that of MAPO-47 at 150 and at 180 °C.

MAPO-B gel. Figure 5 shows the powder patterns obtained in heating the gel from 25 to 200 °C with a constant heating rate of 1.5 °C min^{-1}. The gel is X-ray amorphous at room temperature. At ca. 65 °C a precursor phase is formed. It has a *d*-spacing of 14.9 Å and is not identified. However, this precursor phase disappears again, and the reaction product, MAPO-39, starts to form at ca. 85 °C. At ca. 105 °C new precursor phases start to be formed. Simultaneously, part of the reaction product is consumed, and as the quantity of the precursor phases is increased, the background level of the powder patterns is reduced, indicating consumption of amorphous gel-material in the sample. The new precursor phases are reduced in quantity and disappear at ca. 125 °C, and

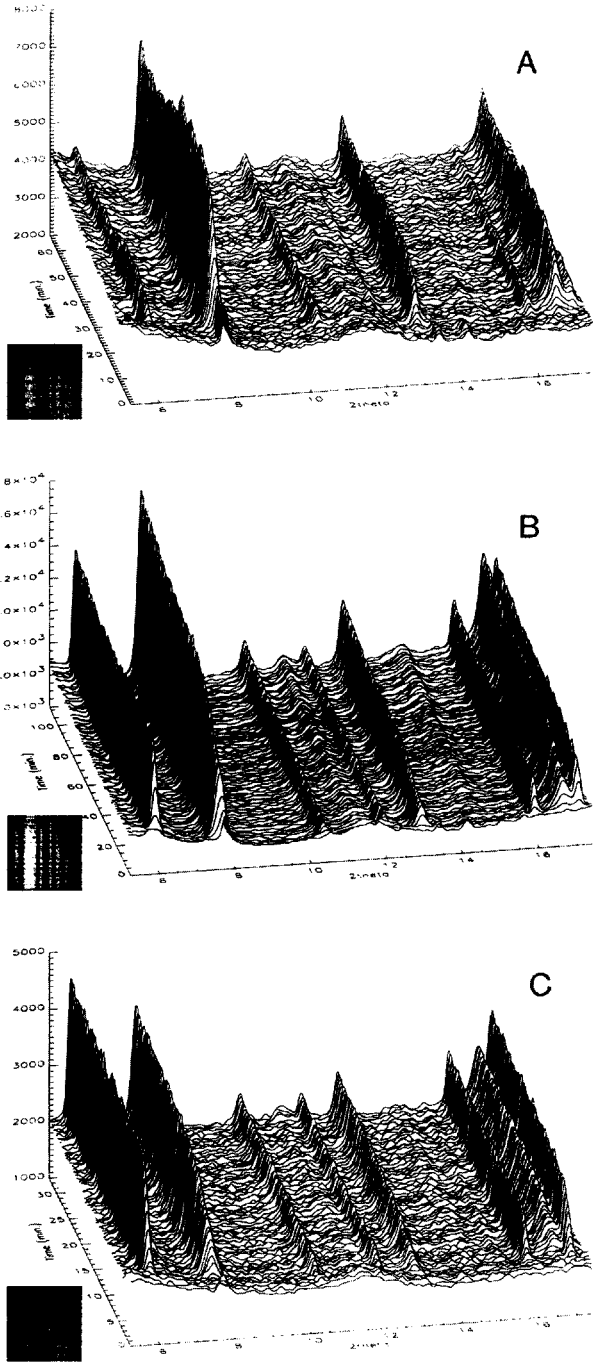

Fig. 3. (A) Patterns of the MAPO-A gel, rapidly heated to 130 °C and kept at this temperature. MAPO-47 is the main reaction product, and MAPO-5 is formed in minor quantities and is partly consumed. (B) Patterns of the gel rapidly heated to 150 °C and kept at this temperature. The rate of formation of MAPO-5 is greater than that of MAPO-47, and the quantity of MAPO-47 formed is greater than that of MAPO-5. (C) Patterns of the gel rapidly heated to 180 °C and kept at this temperature. The rate of formation of MAPO-5 is greater than that of MAPO-47, and the two compounds are formed in approximately equal quantities.

simultaneously increases the quantity of the reaction product. The precursor phases are most likely MAPO-54 with the strong reflection at $d=16.7$ Å, with traces of

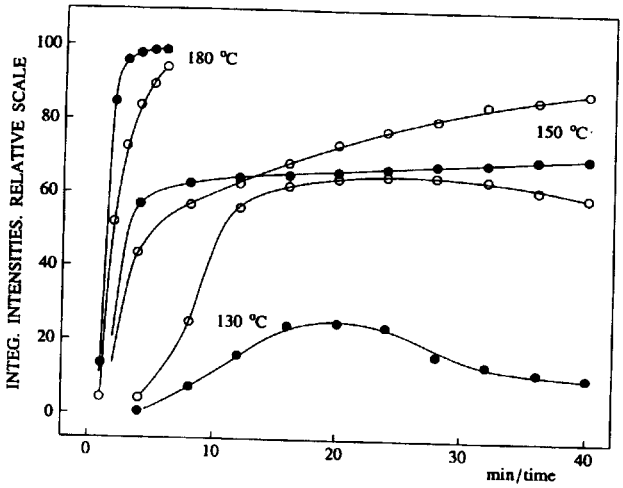

Fig. 4. Integrated intensities of the 100 reflection of MAPO-5, filled circles, and the 101 reflection, open circles, of MAPO-47 at the temperatures 130, 150, and 180 °C, respectively.

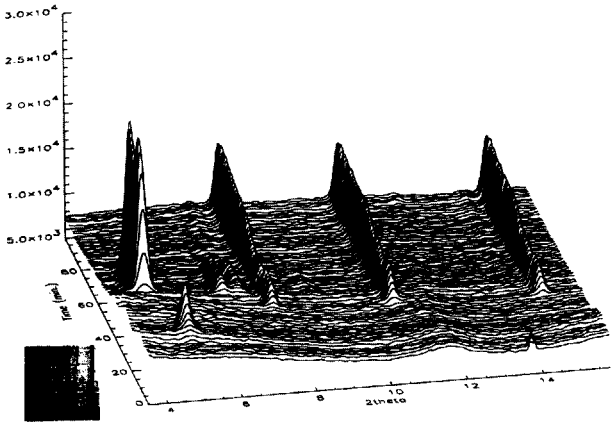

Fig. 5. Patterns of the MAPO-B gel heated from 25 to 200 °C in 60 min and kept at 200 °C for 60 min. The strong Bragg reflection of the precursor VPI-5 is the 100 reflection. The product at 200 °C is MAPO-39 with the 110, 200 and 101 reflections, respectively.

MAPO-5 and MAPO-11, and the reaction product is MAPO-39. MAPO-54 is hexagonal, space group $P6_3$, with $a=18.5$, $c=8.4$ Å, and is a large-pore molecular sieve. MAPO-39 is a small-pore molecular sieve, it is tetragonal, space group $I\bar{4}$, with $a=13.1$, $c=5.2$ Å.

When a sample of the gel is heated to 70 °C and kept at this temperature for 3 h, two crystalline reaction products are formed. The reaction product formed first is the first precursor phase observed in Fig. 5, and the reaction product formed in a slightly slower rate is the Mg-sinkankasite.

Sample of the gel heated to 120 °C and kept at this temperature for 2 h: After approximately 25 min (Fig. 6) weak reflections of MAPO-39 appear, but no significant increase in the quantity of MAPO-39 of the sample is observed. After ca. 40 min, Bragg reflection of a cubic phase starts to appear, and this phase continues to increase in quantity during the rest of the experiment.

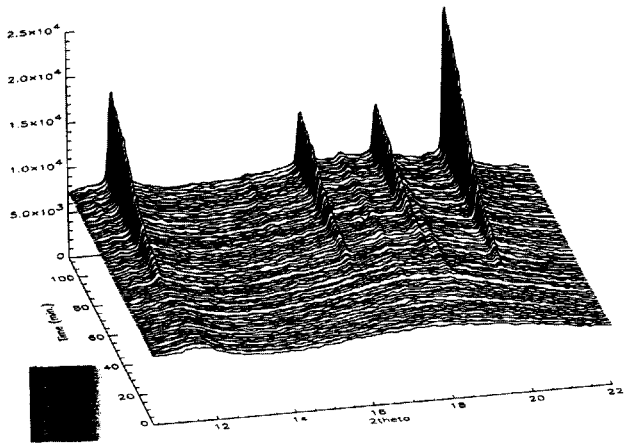

Fig. 6. Patterns of MAPO-B gel kept at 120 °C for 120 min. The strong reflections are the 110, 200, 210 and 211 reflections, respectively, from MAPO-20.

The phase has a powder pattern similar to that of the JCPDS card no. 43-569 (unindexed pattern of a cubic phase).[1] It has most likely a sodalite like structure with $a = 8.89$ Å and is assumed to be MAPO-20.

Sample of the gel heated to 130 °C and kept at this temperature for 3 h: Formation of crystalline materials starts after ca. 5 min (Fig. 7). The first crystalline phase formed increases rapidly in quantity to its maximum value. This phase is MAPO-39. The second crystalline phase formed increases in quantity somewhat slower but increases in quantity during the whole experiment. This phase is assumed to be MAPO-54.

Sample of the gel heated to 200 °C and kept at 200 °C for 0.5 h: The formation of crystalline reaction products starts after ca. 1 min. Two phases are formed with a slightly different growth rate. After ca. 5 min the formation of a third crystalline phase is observed, which, however, disappears again during the following 25 min. This phase is assumed to be MAPO-54. The one phase of the two, formed in the beginning of the experiment, which has the fastest growth rate, has a powder pattern similar to $AlPO_4$-5, and is assumed to be MAPO-5, and the phase which has the slowest growth rate is MAPO-39. The crystallisation of the MAPO-B gel at hydrothermal conditions is thus rather complicated. The composition and growth rate of the product phases are strongly dependent upon the reaction temperature applied. Figure 8 shows the growth rate of MAPO-39 and of MAPO-54 at 130 and 200 °C, respectively.

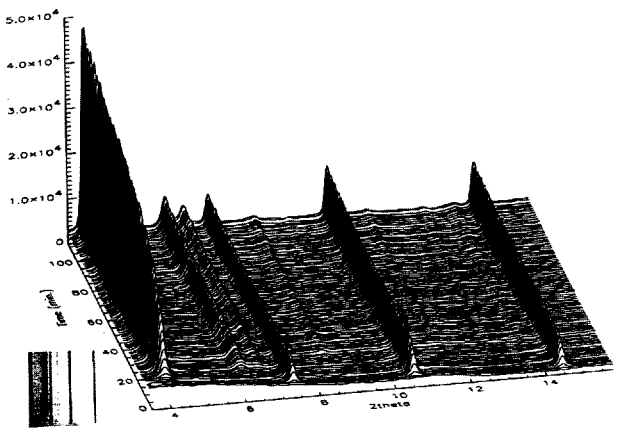

Fig. 7. Patterns of MAPO-B gel kept at 130 °C for 180 min. The reaction products are MAPO-54 and MAPO-39. The four sharp Bragg reflections are: The first the 100 reflection from MAPO-54, and the remaining three the 110, 200 and 101 reflections of MAPO-39. The two broad Bragg reflections observed in the 2θ interval 6–7° are not identified.

MAPO-C gel. This gel has a higher content of the template and of magnesium than the MAPO-B gel. Figure 9 shows the powder patterns obtained in heating the gel from 25 to 200 °C with a constant heating rate of 1.5 °C min^{-1}. At ca. 80 °C the precursor phase MAPO-54 starts to form, but this phase is rapidly consumed at ca. 175 °C, where the reaction products start to be formed.

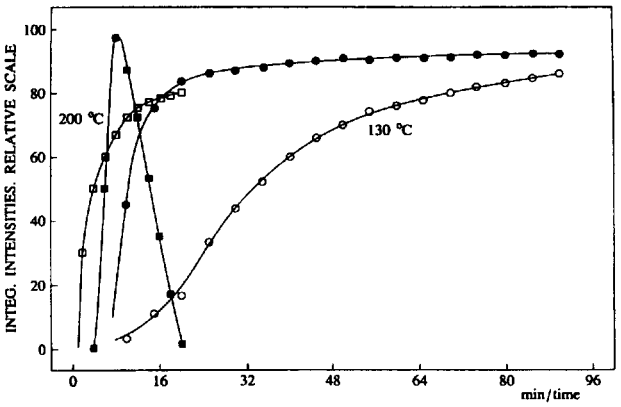

Fig. 8. Growth rate of MAPO-39, open symbols, and MAPO-54, filled symbols, at 130 and 200 °C, respectively, obtained from integration of selected Bragg reflections of the two compounds.

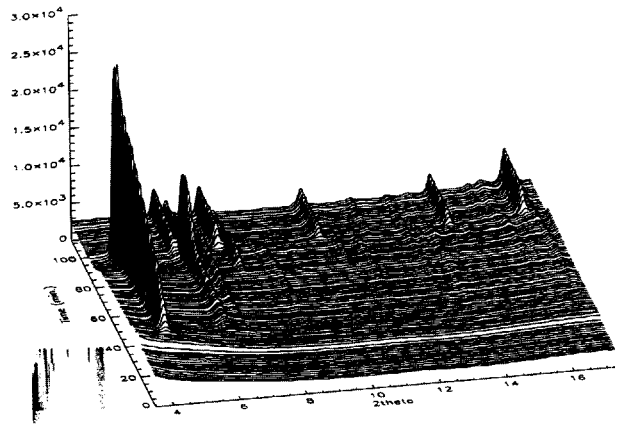

Fig. 9. Patterns of the MAPO-C gel heated from 25 to 200 °C for 120 min. The precursor phase MAPO-54 is consumed at ca. 175 °C. Other precursors, most likely MAPO-5 and MAPO-11, are observed in the temperature range 120–150 °C. The reaction product is a mixture of MAPO-39 and MAPO-46. The four strong Bragg reflections of the reaction product in the 2θ range 7–17° are, from left to right, the 110, 200, 101 and 310 reflections of MAPO-39.

Other precursor phases are formed in the temperature range 120–150 °C, most likely MAPO-11 but they disappear at ca. 150 °C, when the reaction products start to be formed. The reaction product is a mixture of MAPO-39 and MAPO-46. MAPO-46 is a small-pore molecular sieve, it is trigonal, space group $P3c1$ with $a=13.3$, $c=26.9$ Å, using the hexagonal setting.

Samples of the gel were heated to 70 °C and kept at this temperature for 4 h, and were heated to 110 °C and kept at 110 °C for 3 h. Figures 10A and 10B show that only the precursor phase MAPO-54 is formed. A sample of the gel heated to 130 °C and kept at this temperature for 2 h, shows that MAPO-54 is formed immediately (Fig. 10C). After ca. 40 min, Bragg reflection from a second phase most likely MAPO-11 starts to appear. A sample of the gel heated to 150 °C and kept at this temperature for 1 h shows the formation of MAPO-54 and after 10 min also Bragg reflections from the second phase, MAPO-11. A sample of the gel was heated to 180 °C and kept at this temperature for 1 h. The first precursor phase MAPO-54 appeared immediately. After a few minutes Bragg reflection from a new phase appeared. This phase is most likely the final reaction product. The precursor phase was slightly consumed during the formation of this phase.

Sample of the gel heated to 200 °C and kept at 200 °C for 0.5 h. The precursor phase is formed immediately but disappears rapidly during the formation of the final product. The final product is a mixture of MAPO-46 and MAPO-39, with MAPO-46 as the main product. Figure 11 displays integrated intensities of the first reflection in the precursor MAPO-54 vs. time at three temperatures, showing how the rate of formation increases with increasing temperature.

The *in-situ* experiments with the MAPO-C gel at hydrothermal conditions show as with the MAPO-B gel that it is possible to obtain different reaction products in dependence of the reaction temperature. In the two gels, the organic template was di-*n*-propylamine.

MAPO-D gel. This gel was made with tripropylamine as the template and with a template concentration and a $MgO:Al_2O_3$ ratio similar to the gels used by Alkolekar[8] in the synthesis of MAPO-36. Figure 12 shows the powder patterns obtained in heating the gel from 25 to 200 °C with a constant heating rate of 1.5 °C min^{-1}. The gel is X-ray amorphous at 25 °C and no precursor phases are formed on heating. At ca. 100 °C Bragg reflection of the crystalline reaction product starts to form. This reaction product is MAPO-36. Simultaneously, the background of the X-ray patterns is reduced considerably indicating consumption of amorphous material. A final reaction product is formed over 170 °C in this experiment under consumption of MAPO-36. However, it was not possible in later experiments to reproduce the formation of this phase. The compound is most likely formed due to a leak in the capillary, and the two strong reflections in its powder pattern at $d=4.37$ and $d=4.14$ Å correspond to the first two strong lines in the powder pattern of $AlPO_4$, JCPDS card no. 20–45.[14] MAPO-36 has medium size pores. It is monoclinic, space group $C2/c$ with $a=13.1$, $b=21.6$, $c=5.2$ Å and $\beta=92°$.

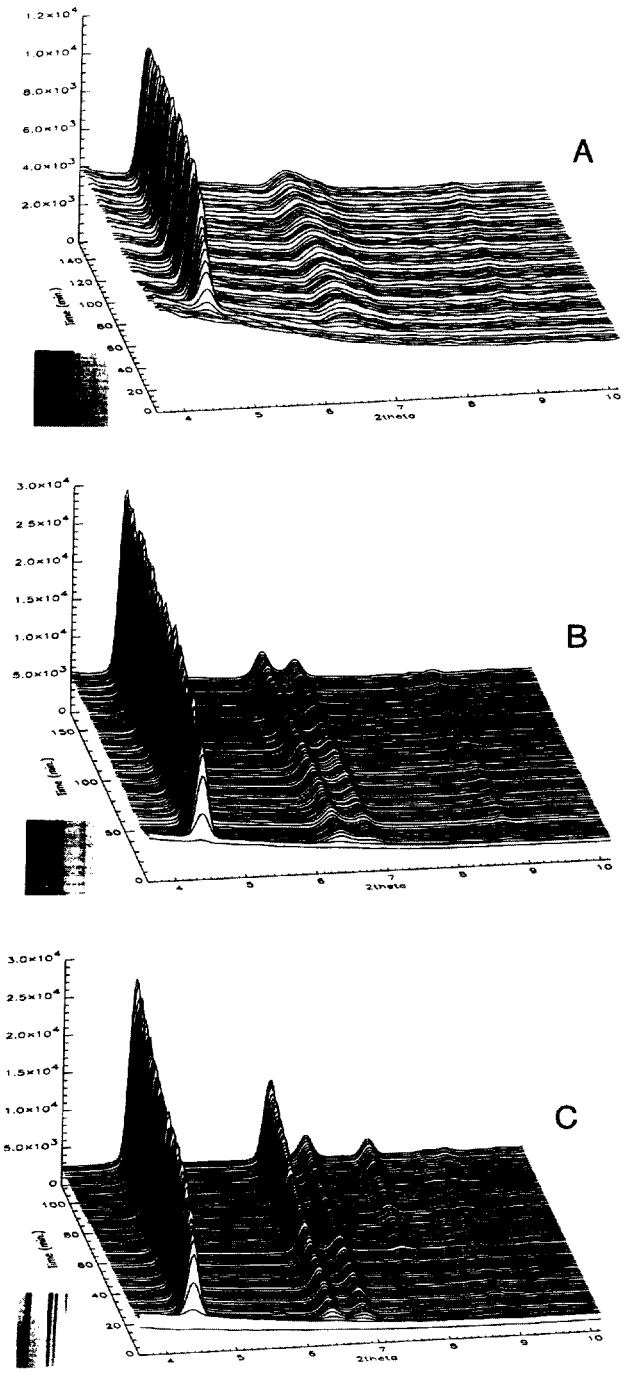

Fig. 10. (A) Patterns of the MAPO-C gel rapidly heated to 70 °C and kept at this temperature. The reaction product is MAPO-54. (B) Patterns of the gel rapidly heated to 130 °C and kept at this temperature. (C) Patterns of the gel rapidly heated to 150 °C and kept at this temperature. The reaction products are MAPO-54 and MAPO-11. The Bragg reflections at the 2θ values 6.5 and 7.6° are the 110 and the 020 reflections of MAPO-11.

The gel was heated to 70 °C and kept at 70 °C for 3 h.

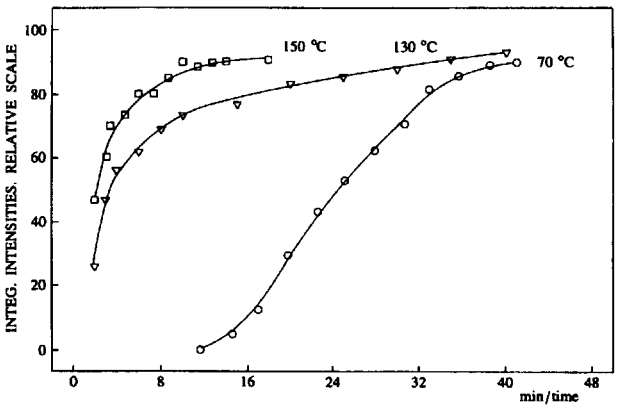

Fig. 11. Growth rate of MAPO-54 at three temperatures obtained from integration of the 100 reflection of the compound. Only at 70 °C is a sigmoidal shape of the growth curve observed.

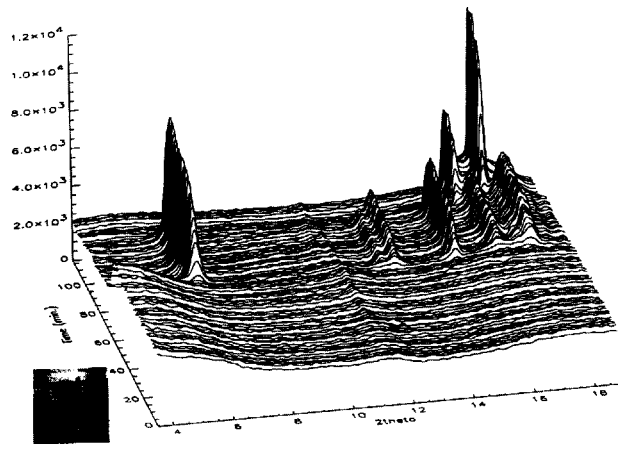

Fig. 12. Patterns of the MAPO-D gel heated from 25 to 200 °C for 120 min. The first phase formed is MAPO-36. The second phase formed is an aluminium phosphate, the two strong reflections in the upper right part of the patterns and is most likely formed due to a pressure leak of the capillary. The six Bragg reflections of the MAPO-36 diagrams have the following Miller indices: 110, 220, 040, −111, 310 and −131, respectively.

Only diffuse lines were observed in the X-ray patterns, and no crystalline phases were formed. Other samples of the gel were heated to 130 °C and kept at that temperature for 1 h (Fig. 13) and to 150 °C for 0.5 h. The crystalline reaction products were in these two cases MAPO-36. The rates of formation of MAPO-36 at the two temperatures are displayed in Fig. 14. Finally, a gel was heated to 190 °C and kept at 190 °C for 0.5 h. The main product of the crystalline reaction product formed was MAPO-36.

MAPO-E gel. This gel was made with tetramethylammoniumhydroxide as the template. Fig. 15 shows the powder patterns obtained on heating the gel from 25 to 200 °C with a constant heating rate of 1.5 °C min^{-1}. A precursor phase is formed in the temperature range 25–80 °C. This phase is Mg-sinkankasite. The precursor phase is consumed in the formation of the product that starts to

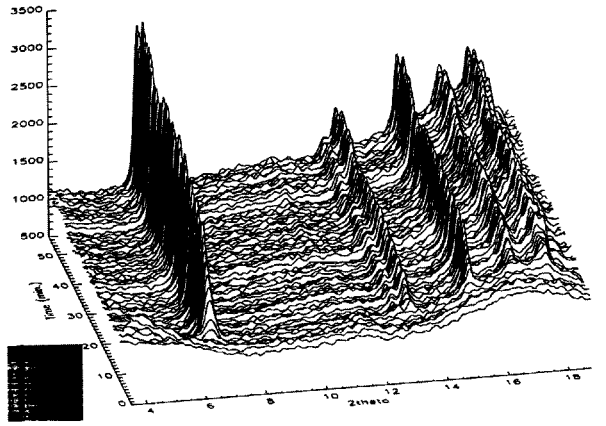

Fig. 13. Patterns of the MAPO-D gel rapidly heated to 130 °C and kept at this temperature. The reaction product is MAPO-36.

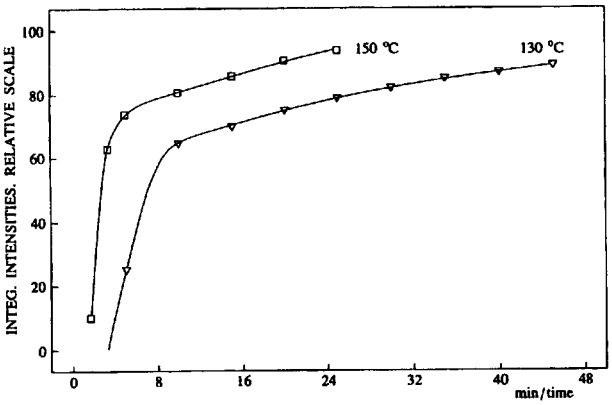

Fig. 14. Growth rate of MAPO-36 at two temperatures from integration of the 110 reflection of the powder patterns.

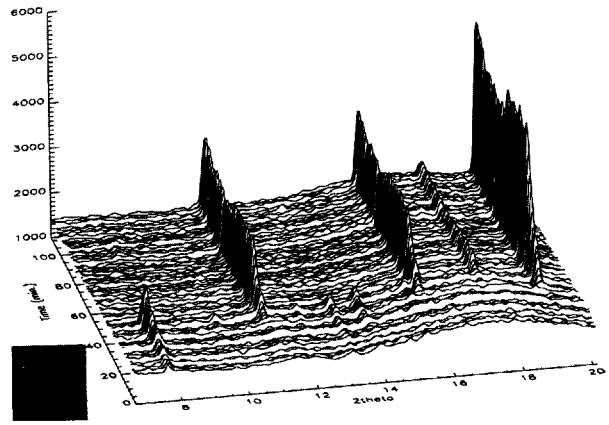

Fig. 15. Patterns of the MAPO-E gel heated from 25 to 200 °C for 120 min. The precursor phase formed is Mg-sinkankasite and the reaction product is MAPO-20. The four Bragg reflections of the powder patterns of the reaction product are the 110, 200, 210 and 211 reflections, respectively, of MAPO-20.

appear at ca. 65 °C. The product is a sodalite-like phase, MAPO-20 with a powder pattern similar to $AlPO_4$-20, JCPDS card no. 43–569.[1] MAPO-20 is a small-pore

molecular sieve. The structure is cubic, $a=9.0437$ Å, space group $Pm\bar{3}n$. A gel was heated to 50 °C and kept at 50 °C for 3 h (Fig. 16). Mg-sinkankasite was formed immediately and no other phases were formed. A gel heated to 75 °C and kept at this temperature for 2 h showed immediate formation of Mg-sinkankasite which was slightly consumed during the experiment. The cubic sodalite phase MAPO-20 starts to form at the beginning of the experiment and increases in quantity during the time of the experiment.

A gel was heated to 90 °C and kept at 90 °C for 8 h (Fig. 17). Mg-sinkankasite is formed fast but is also consumed fast in the formation of the reaction product MAPO-20. The same trend was observed for gels heated to and kept at 105 °C for 3 h and to 120 °C for 3 h. Figure 18 displays the growth and consumption rate of Mg-sinkankasite and the growth rate of MAPO-20 at the five temperatures investigated.

Conclusion

The results of the *in-situ* experiments with the MAPO-gels at isothermal hydrothermal conditions are listed in

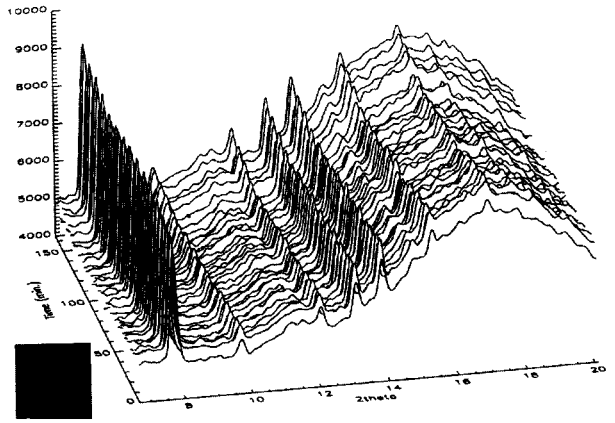

Fig. 16. Patterns of the MAPO-E gel heated rapidly to 50 °C and kept at this temperature. The reaction product is Mg-sinkankasite.

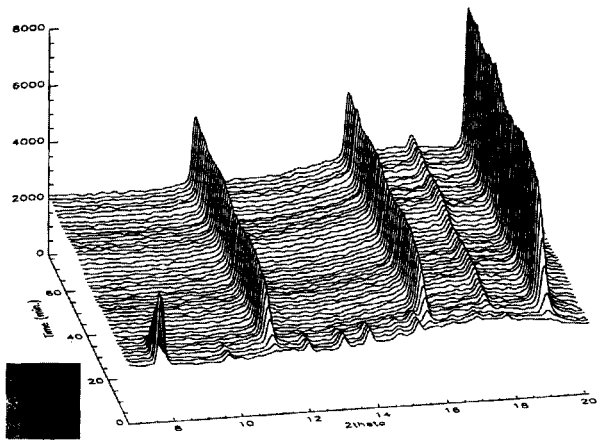

Fig. 17. Patterns of the MAPO-E gel heated rapidly to 90 °C and kept at this temperature. The reaction product is MAPO-20.

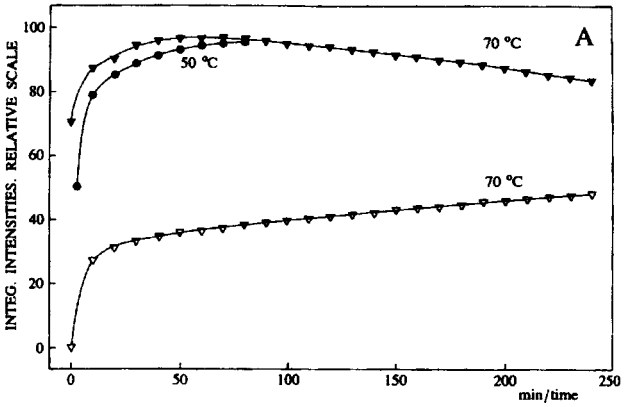

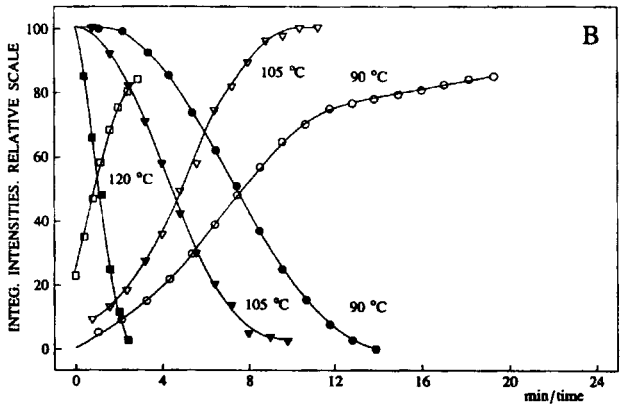

Fig. 18. (A) Growth rate of Mg-sinkankasite, filled symbols, at 50 and 70 °C, respectively, and of MAPO-20, open symbols, at 70 °C. (B) Growth rate of MAPO-20 at 90, 105 and 120 °C, open symbols, and rate of consumption of Mg-sinkankasite at the same temperatures, filled symbols.

Table 3. The experiments on the five MAPO-gels show that the formation of the products, the MAPOs 5, 20, 39, 46 and 47, may pass through the formation of precursor and intermediate phases, and that only the formation of MAPO-36 in this case proceeded without a precursor. A precursor is not present in the reaction product, and an intermediate phase is partly consumed and present in the reaction product. The formation of Mg-sinkankasite as a precursor or intermediate phase has not been reported previously. It is not clear why it does not occur in all the MAPO gels investigated. It could depend upon the pH value of the gel. However, this has not been investigated. As reported earlier a selection of reaction products may be obtained with di-*n*-propylamine as the template, and this is also the case in the *in-situ* experiments with the gels MAPO-B and -C (Table 3). However, with these gels, the hydrothermal experiments in the pressure vessels yielded the MAPO-39 compound (Table 2). The differences between the composition of the reaction products when using a pressure vessel with a glass or Teflon liner, or performing the reactions in the *in-situ* experiments in quartz capillaries

Table 3. Results of *in-situ* experiments with MAPO-gels, isothermal conditions.

Gel	Aging time[a]/ days	Hydrothermal T/°C	Precursor phase	Intermediate phases	Reaction products
MAPO-A	44	130	Mg-sinkankasite	MAPO-5	MAPO-47
		150			MAPO-47, MAPO-5
		180			MAPO-47, MAPO-5
MAPO-B	24	70	Unidentified comp.		Mg-sinkankasite
		120		MAPO-39	MAPO-20
		130			MAPO-39, MAPO-54
		200		MAPO-54	MAPO-39, MAPO-5
MAPO-C	6	70			MAPO-54
		110			MAPO-54
		130			MAPO-54, MAPO-11
		150			MAPO-54, MAPO-11
		180		MAPO-54	MAPO-46, MAPO-39
		200		MAPO-54	MAPO-46, MAPO-39
MAPO-D	6	70			X-ray amorphous
		130			MAPO-36
		150			MAPO-36
		190			MAPO-36
MAPO-E	6	50			Mg-sinkankasite
		75		Mg-sinkankasite	MAPO-20
		90	Mg-sinkankasite		MAPO-20
		150	Mg-sinkankasite		MAPO-20
		120	Mg-sinkankasite		MAPO-20

[a] Aging time at room temperature prior to *in-situ* experiments.

may well be ascribed to different heating rates, which are of the order of 1 h for the pressure vessel and <5 min in the *in-situ* experiments. Composition and aging history of the gels, aging processes which proceed during a slow heating of the sample, are assumed to influence the reaction paths and thus resulting in different compositions of the reaction products (Tables 2 and 3).

Table 4 lists the structure code,[15] ring size, pore size and crystallographic data for the identified MAPO compounds and their model compounds. It is interesting to note that with the MAPO-A gel the formation of the product MAPO-5 with a 12-ring is faster than the formation of the product MAPO-47 with an 8-ring (Fig. 2). With the MAPO-B gel the formation of the precursor phase MAPO-54 with an 18-ring is faster than the formation of the product MAPO-39 with an 8-ring (Fig. 5), and this is also the case in the use of the MAPO-C gel (Fig. 9). The use of the MAPO-D and the MAPO-E gels did not result in precursor phases with molecular sieve character.

The well known techniques from the *in-situ* neutron powder diffraction analysis of the dynamic processes occuring during hydrothermal synthesis[16,17] have been developed for the study of *in-situ* zeolite synthesis using synchrotron radiation. The *in-situ* diffraction experiments can be performed in an energy dispersive mode[18–22] or

Table 4. Compounds identified and their model compounds with structural data.[15]

Phase identified	Structure code	Model compound	Ring size	Pore size/Å	Space group	Unit cell parameters			
						a/Å	b/Å	c/Å	β/Å
MAPO-5	AFI	$AlPO_4$-5	12	7.3, 7.3	$P6cc$	13.7		8.4	
MAPO-11	AEL	$AlPO_4$-11	10	6.3, 3.9	$Imma$	8.4	18.5	13.5	
MAPO-20	SOD	$AlPO_4$-20	6		$P\bar{4}3n$	8.9			
MAPO-36	ATS	MAPO-36	12	6.5, 7.5	$C2/c$	13.1	21.6	5.2	92
MAPO-39	ATN	MAPO-39	8	4.0, 4.0	$I4$	13.1		5.2	
MAPO-46	AFS	MAPSO-46	12	6.2, 6.2	$P3c1$	13.3		26.9	
MAPO-47	CHA	Chabazite	8	3.8, 3.8	$R\bar{3}m$	13.2		15.1	
MAPO-54	VFI	VPI-5	18	12.1	$P6_3$	18.5		8.4	

in a monochromatic mode.[5] *In-situ* solid state NMR has also been used to study the real-time synthesis of a zeolite.[23] The present *in-situ* investigation of magnesium aluminophosphate synthesis shows that detailed information may be obtained about the synthesis by the use of monochromatic synchrotron X-ray powder diffraction.

Acknowledgements. The Danish Natural Science Research Council has supported this investigation with grants. The synchrotron X-ray measurements were carried out at Brookhaven National Laboratory, supported under contract DE-AC02-76CH00016 with the US Department of Energy by its Division of Chemical Sciences Office of Basic and Energy Science. Mrs. M. A. Chevallier, Mrs. C. Secher, Mr. A. Lindahl and Mr. N. J. Hansen are acknowledged for valuable assistance.

References

1. Wilson, S. T., Lok, B. M. and Flanigen, E.M. U.S. Pat. 4310440 (1982).
2. Ojo, A. F. and McCusker, L. B. *Zeolites 11* (1991) 460.
3. Akolekar, D. B. and Kaliaguine, S. K. *Zeolites 14* (1994) 620.
4. Flanigen, E. M., Lok, B. M., Patton, R. L. and Wilson, S. T. *Stud. Surf. Sci. Catal. 28* (1986) 103.
5. Norby, P., Christensen, A. N. and Hanson, J. C. In Weitkamp, J., Karge, H. G., Pfeifer, H. and Hölderich, W. (Eds.). *Zeolites and Related Microporous Materials: State of the Art 1994. Studies in Surface Science and Catalysis 84* (1994) 179.
6. Shea, W.-L., Borade, R. B. and Clearfield, A. *J. Chem. Soc., Faraday Trans. 89* (1993) 3143.
7. Akolekar, D. B. and Kaliaguine, S. *J. Chem. Soc., Faraday Trans. 89* (1993) 4141.
8. Akolekar, D. B. *J. Catal. 143* (1993) 227.
9. Han, S., Smith, J. V., Pluth, J. J. and Richardson Jr., J. W. *Eur. J. Mineral. 2* (1990) 787.
10. Christensen, A. N., Norby, P., Hanson, J. C. and Shimada, S. *J. Appl. Crystallogr. 29* (1996) 265.
11. Burns, P. C. and Hawthorne, F. C. *Am. Mineral. 80* (1995) 620.
12. Yvon, K., Jeitschko, W. and Parthé, E. *J. Appl. Crystallogr. 10* (1977) 73.
13. Barrie, P. J. and Klinowski, J. *J. Phys. Chem. 93* (1989) 5972.
14. Flörke, O. W. *Z. Kristallogr. 125* (1967) 134.
15. Meier, W. M. and Olson, D. H. *Atlas of Zeolite Structure Types*, 3rd Rev. Edn. Butterworth-Heinemann, London 1992.
16. Christensen, A. N. and Lehmann, M. S. *J. Solid State Chem. 51* (1984) 196.
17. Polak, E., Munn, J., Barnes, P., Tarling, S. E. and Ritter, C. *J. Appl. Crystallogr. 23* (1990) 258.
18. Barnes, P., Hausermann, D. and Tarling, S. E. *Inst. Phys. Conf. Ser. 111* (1990) 61.
19. He, H., Barnes, P., Munn, J., Turillas, X. and Klinowski, J. *Chem. Phys. Lett. 196* (1992) 267.
20. Munn, J., Barnes, P., Hausermann, D., Axon, S. A. and Klinowski, J. *Phase Transitions 39* (1992) 129.
21. Evans, J. S. O., Francis, R. J., O'Hare, D., Price, S. J., Clark, S. M., Flaherty, J., Gordon, J., Nield, A. and Tang, C. C. *Rev. Sci. Instrum. 66* (1995) 2442.
22. Rey, F., Sankar, G., Thomas, J. M., Barrett, P. A., Lewis, D. W., Catlow, C. R. A., Clark, S. M. and Greaves, G. N. *Chem. Mater. 7* (1995) 1435.
23. Shi, J., Anderson, M. W. and Carr, S. W. *Chem. Mater. 8* (1996) 369.

Received March 8, 1996.